Spring 2014

Study of the e/pi ratio for the shashlik detector via simulated proton collision events

Spencer C. Jones
spencerjones626@yahoo.com

THE FLORIDA STATE UNIVERSITY
COLLEGE OF ARTS AND SCIENCES

STUDY OF THE E/π RATIO FOR THE SHASHLIK DETECTOR

VIA SIMULATED PROTON COLLISION EVENTS

By

Spencer Jones

A Thesis submitted to the Department of Physics

in partial fulfillment of the requirements for

graduation with Honors in the Major

Degree Awarded:

Spring, 2014

The members of the Defense Committee approve the thesis of Spencer Jones defended on April 15, 2014

X

Dr. Todd Adams
Thesis Director

X

Dr. Mark Sussman
Outside Committee Member

X

Dr. Horst Wahl
Committee Member

Contents

Abstract

The intention of this research project was to calculate the e/π ratio for the proposed Shashlik Detector for the Compact Muon Solenoid Experiment by simulating proton collision events in a virtual detector. The e/π ratio is the ratio of the Shashlik's ability to measure the energy of electromagnetic to hadronic particles. An upgrade is required for the electromagnetic calorimeter due to radiation damage of the current detector. The Shashlik Detector is a potential replacement for the current $PbWO_4$ electromagnetic calorimeter and is designed with a layered pattern of scintillating material and absorber. I have analyzed this ratio for various absorber and scintillator thicknesses to determine the best ratio of materials to use.

Part 1: Introduction

Motivation

When the Large Hadron Collider was completed in 2008, the Compact Muon Solenoid (CMS) detector, one of the two general purpose detectors, began its journey of being one of the largest experiments in human in history. Since the beginning of operations, trillions of protons have collided in the detector and, as such, has given us significant insight into areas including large extra dimensions, supersymmetry [1], and of course the Higgs boson [2]. However, the strain on the detector has been extreme and the electromagnetic calorimeter (ECAL) has been damaged over time. Eventually, part of the CMS detector will become inoperational and need to be replaced. One of the options for replacement is the Shashlik Detector. This detector has several qualities that improve on the original but needs to be studied before it can be implemented. The goal of this thesis is to determine the ratio of response of the Shashlik detector to electrons versus the response to pions (e/π ratio) using simulations; and in doing so, help determine some of the specifications of the detector.

The CMS Detector

The CMS detector is built in a layered fashion with each layer able to detect different particles or different aspects of particles [3]. It is built in a barrel shape with proton-proton collisions happening in the center with the products of these collisions moving outward through the barrel and end caps. These particles first pass through the silicon tracker where the physical path of charged particles can be accurately measured. Immediately behind the tracker are the electromagnetic and hadronic calorimeters where the energy of electromagnetic particles (electrons and photons) and hadrons (quark-based particles) can be measured, respectively. By this point in the detector, the majority of particles from the proton collisions have been absorbed by the calorimeters leaving only muons and neutrinos. The muons pass through the superconducting magnet on their way to be measured by the outermost part of the detector, the muon system, while the elusive neutrinos escape and must be inferred using methods like momentum conservation.

Part 2: Background

Section 2.1: How Particles are seen

Electromagnetic calorimeters are usually made of scintillating materials that output light when in the presence of a charged particle. The intensity of this light is proportional to the energy of the particles incident on the detector. This allows for analysis of the various charged particles that are produced in proton collisions. Scintillators can also measure neutral particles as soon as they interact with the medium or decay via the weak force; both of which can produce charged particles as explained in the non-charged particles section below.

Scintillation

When a charged particle passes through a scintillating material, it transfers some of its energy to the electrons via the electromagnetic force [4]. This increase of energy for the electron brings it to an excited state where it remains for a short time before decaying back to the ground state. When the electron returns to the lower energy ground state, a photon is released. This photon reflects around in the material until being read out by photoelectric diodes and thus the charged particle's presence is known. After exciting one electron, a passing charged particle will excite other electrons until it runs out of energy and is absorbed completely in the material, interacts with the material and showers new particles, or punches through the calorimeter and into the next part of the detector. Higher energy particles excite more electrons and shower into more particles, thus more photons are emitted. This allows experimenters to determine how much energy the initial particle had by analyzing the intensity of the light pulse [5].

Decay Time

All scintillating materials work in the way explained above; however different materials have different properties. An important property is the decay time of the scintillator. This measures how quickly a scintillator can measure new events and is defined by the amount of time it takes for the intensity of a light pulse to return to 1/e of its maximum value. Short decay times are important for experiments like at the LHC where many events take place every second [3].

Non-Charged Particles

Scintillators can only measure charged particles but there are there also neutral particles that need to be measured. Fortunately, the neutral particles either decay or interact with the medium to create charged particles that can then be measured. Photons, for example, cannot ionize electrons independently but instead undergo pair production where an electron and an anti-electron (positron) are created. Both of these resultant particles are charged and can easily transfer their energy to the material's electrons. It is important to note that pair-production can only occur when in the presence of a nucleus to refrain from violating energy conservation. Fortunately, there are plenty of nuclei in detectors for this to occur. Lower energy photons can also interact via Compton scattering and the photoelectric effect with electrons in the medium. This process transfers some of the photon's energy to the electron but keeps the photon intact where it can then interact with another electron or produce an electron/positron pair. Pions either interact via strong interactions with the medium which cause particles to shower (as described below) or decay into other particles. For example, neutral pions (π^0) decay into two photons as in equation 1.1.

$$\pi^0 \rightarrow \gamma\gamma \qquad [1.1]$$

Either way, new particles are created and will either cause the material to scintillate (if they are charged) or will interact with the medium to create new particles. Eventually, all particles are absorbed or escape the calorimeter.

The distance that these particles travel before being completely absorbed is a well-defined quantity for both electromagnetic and hadronic particles. For electromagnetic particles, the term “radiation length” is given to the distance at which electron can travel before losing all but 1/e of its energy by means of bremsstrahlung radiation. Similarly, the interaction length is defined by the distance a particle can travel before losing all but 1/3 of its energy via nuclear interactions [5].

Particle Showers

The presence of a medium usually causes high energy particles to shower into many new particles. This can occur electromagnetically or by nuclear interactions. Electromagnetic showers develop via two well-known processes. High energy electrons (> ~10 MeV) primarily lose their energy by bremsstrahlung radiation and photons of similar energy undergo pair-production. Bremsstrahlung radiation creates new photons while pair-production creates new electrons and positrons. These resultant particles have lower energies than their ancestors but will continue to create new particles by the same means until the energy of the showering particles falls below some critical energy. This critical energy is defined by the energy at which particles will lose the rest of their energy via ionization, excitation, and the photo-electric effect and not in the generation of new particles. The result of all these new particles is a shower of electrons and photons whose energy is lower the longer the shower develops. The width of the shower is given by the Molière radius which is defined as the average lateral deflection of particles at the critical energy after they travel one radiation length. The Molière radius is intrinsic to the materials that make up the detector and needs to be small for high energy experiments to maximize resolution.

Nuclear showers are largely less understood than electromagnetic showers. Hadronic particles interact with nuclei to create new quark based particles with lower energy. Many of these particles will be pions and due to the charge independence of hadronic interactions in each collision, about a third of these pions will be neutral pions. These neutral pions will then decay into photons as in equation 1.1 which will then interact electromagnetically as described above. The rest of the hadronic particles will continue to interact with nuclei until a shower develop. Unfortunately, there is usually more energy loss in hadronic showers due to energy loss via nuclear processes such as nucleon evaporation and spallation. This usually causes detectors to read out more electromagnetic energy than hadronic and thus the e/π ratio is usually greater than 1.

Crystal Impurities

All bound electrons can only exist within a series of energy levels determined by the nucleus and other electrons. This means that passing particles can only excite electrons into certain energy levels and these electrons can only drop a pre-defined energy. This phenomenon not only increases the decay time but also prevents some energy transfer if the particles to be measured do not have the correct energy. This problem is overcome by introducing an impurity into the scintillating crystal. By “doping” the crystal, as it called, the material gains extra band gaps that the electrons can fall in to. This allows the electrons to decay to the ground state more quickly and allows for more energy absorption.

Section 2.2: The Detectors

The CMS ECAL

The electromagnetic calorimeter is designed to measure the energy of electromagnetic particles. In the endcap, this is done using thousands of crystals arranged as shown in Figure 2.1. In the barrel, the crystals are oriented in a barrel shape with the smallest face of the crystal on the inside. The crystals are projective so that the incident particles travel through the maximum amount of crystal. Only the crystals in the endcap of the detector are being replaced with a new type of scintillator because the barrel crystals experience much less radiation and therefore are not as damaged. Because of their cross-sections, the majority of beam-line protons scatter at low angles or miss each other entirely. This results in the majority of radiation being located around the beam-line where the endcaps are located [3].

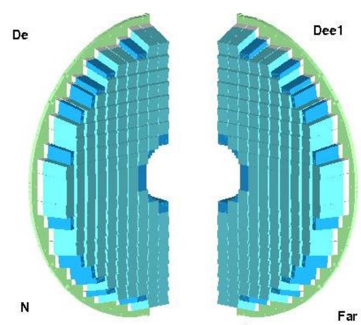

Figure 2.1: This is the current endcap of the CMS ECAL. The $PbWO_4$ crystals are projective so that they all point towards the collision point [5].

$PbWO_4$

The CMS detector currently uses $PbWO_4$ crystals for its electromagnetic calorimeter. This is a solid crystal absorber with a density greater than iron. It was chosen for its role in the CMS detector due to its very low radiation length, fast decay time, and radiation hardness. The radiation length of $PbWO_4$ is actually the lowest among all known scintillators at 0.9 cm and the decay time is a respectable 3-5 ns

[6]. It has relatively low light output compared to other scintillators (especially organic scintillators that have much higher light output) although this is acceptable in high energy environments like the LHC [4]. Unfortunately, $PbWO_4$ is not quite resistant enough to radiation and some of the crystals, especially those in the endcaps, are becoming badly damaged. Some of this damage can be corrected by allowing the crystal to regenerate at higher temperatures during experimental downtime but in the long term this will not be sufficient [7]. By the time of replacement, many crystals are expected to be nearly opaque which significantly cuts down on the light that will reach the photodetectors. This is the primary reason for replacement.

The Shashlik Design

A Shashlik electromagnetic calorimeter is comprised of an alternating series of scintillating material and absorber with readout fibers running perpendicular to the layers. One of the current plans for replacement in the CMS detector is to use tungsten absorber and LYSO (Luetetium Yttrium Orthosilicate) crystals [8]. Tungsten is a very dense metal and as such has a small interaction length making it a good producer of hadronic showers [9]. With tungsten absorber layered throughout, the detector becomes more radiation hard and can absorb more energy thus helping ensure that particles do not escape undetected. Tungsten is also cheaper to produce than scintillating crystal so there is a large cost benefit as well. LYSO is similar to $PbWO_4$ in that it has a short radiation length (1.1 cm) and is very radiation hard. However, compared to $PbWO_4$'s decay time, LYSO crystal has a long decay time of 40 ns [10]. The largest benefit of LYSO is that it is not overly costly so when used in combination with tungsten, each element of the detector will be relatively cheap. The properties of LYSO crystal and tungsten are listed in Table 1.1 and Table 1.2, respectively.

Physical Properties of LYSO

Table 1.1: The physical properties of LYSO crystal as measured by Omega Piezo, a producer of LYSO crystals [10].

Density (g/cm^3)	7.4
Effective Atomic Number	66
Radiation Length (cm)	1.10
Decay Constant (ns)	40-44
Peak Emission (nm)	428
Light Yield (Relative BGO=100%)	190
Index of Refraction	1.82
Peak excitation (nm)	375
Radiation Hardness (rad)	>106
Melting Point (°C)	2050
Hardness (Mohs)	5.8
Cleavage	None
Hygroscopicity	No

Physical Properties of Tungsten

Table 1.2: The physical properties of Tungsten as measured by the Particle Data Group [11].

Quantity	Value
Atomic Number	74
Atomic Mass	183.84 g/mol
Density	19.3 g/cm^3
Mean Excitation Energy	727.0 eV
Minimum Ionization	22.10 MeV/cm
Nuclear Interaction Length	9.95 cm
Radiation Length	0.35 cm
Molière Radius	0.933 cm

A side effect of the absorber layers is that scintillated light cannot travel through the tower due to tungsten's opacity. To overcome this problem, four optical wires run through the tower as shown in Figure 2.2. These will transport the scintillated light through the absorber and be read out the back end. Another fiber runs through the center for calibration and to monitor the tower via lasers.

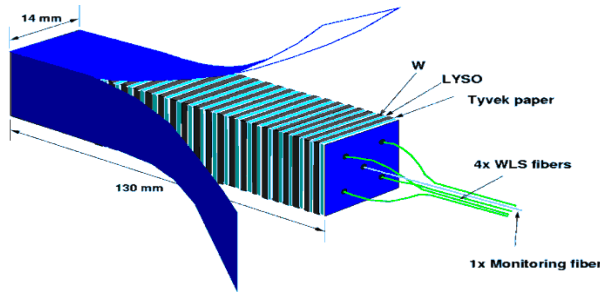

Figure 2.2: A picture of the Shashlik's design. The layers are comprised of LYSO crystal and W absorber. Four optical wires travel through tower to a photo detector at the back and a monitoring fiber penetrates through the middle [8].

Part 3: Analysis

Section 3.1: Experimental Process

To study the e/π ratio, simulations were run using Pythia for particle generation [12] and GEANT4 for detector simulation [13]. Pythia was used to generate separate streams of particles. These streams consisted of 2000 events of single electrons containing a fixed energy were created with the same being done for negative pions. The default constructions of the virtual detector within GEANT's libraries include the $PbWO_4$ detector and the new Shashlik detector but both are designed to replicate the real CMS detector. For these studies this was changed to extend the Shashlik detector to fully contain the energy of a 1 TeV pion so that the only energy loss was due to the properties of the detector and not to energy escaping out the end. With this modification, the generated electrons and pions were propagated through the newly constructed detector and the energy output for both was used to calculate the ratio. An example of this output is given in Figure 3.1 where the energy deposition of an electron is shown.

An important distinction between these simulations and reality is that there is no simulation of light production within the calorimeters. Instead, any energy that would be used to create a scintillation photon is given directly as energy output. Also, GEANT4 tracks particles until they have deposited all their energy into the material; but a production cut-off is included that prohibits the production of new particles from parent particles with less than the cut-off limit. This approach is similar to what occurs in reality in that parent particles cannot produce new particles if the parent's energy is not greater than the combined mass of the new particles but differs in that particles will not always deposit readable energy until they have none. This results in increased error and creates a slight discrepancy between simulation and reality.

Energy Deposition of Electron

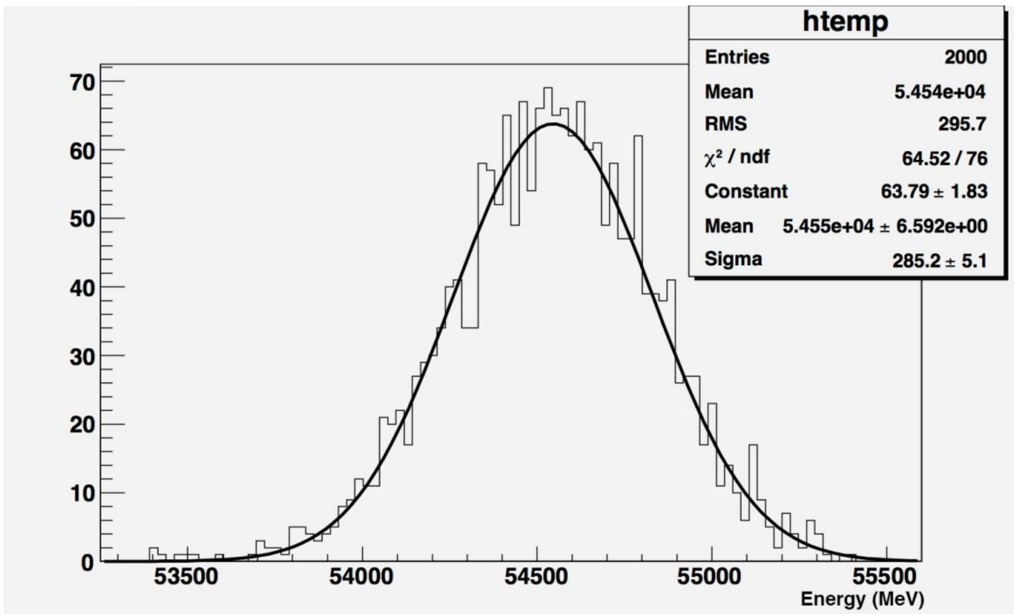

Figure 3.1: This figure shows the energy deposition of electrons with 500 GeV of energy. The x-axis shows energy in MeV and the y-axis sows the number of events in each bin. This was measured using 0.5mm scintillator and 1.5mm absorber. The black line is the Gaussian fit for the deposition.

Various thicknesses of absorber (1.5mm – 3.5 mm with 0.2mm intervals) and scintillating (0.5mm – 2.5mm with 0.2 mm intervals) layers were used as well several different particle energies (5 GeV, 10 GeV, 20 GeV, 50 GeV, 100 GeV, 500 GeV, 1000 GeV). This allows for an analysis of the ratio's dependence on all three quantities. The energy distribution given by GEANT was fit to a Gaussian (as seen in Figure 3.1) and the mean of this fit is used as the energy in this analysis. The ratios of energies found this way for electrons versus pions is used for the e/π ratio.

Section 3.2: Data Analysis

The e/π ratio was calculated for various energies and thicknesses of the absorber/scintillator layers. The data is quite precise with relatively small errors. Plots of the ratio vs varying quantities are given below.

Ratio Vs Energy

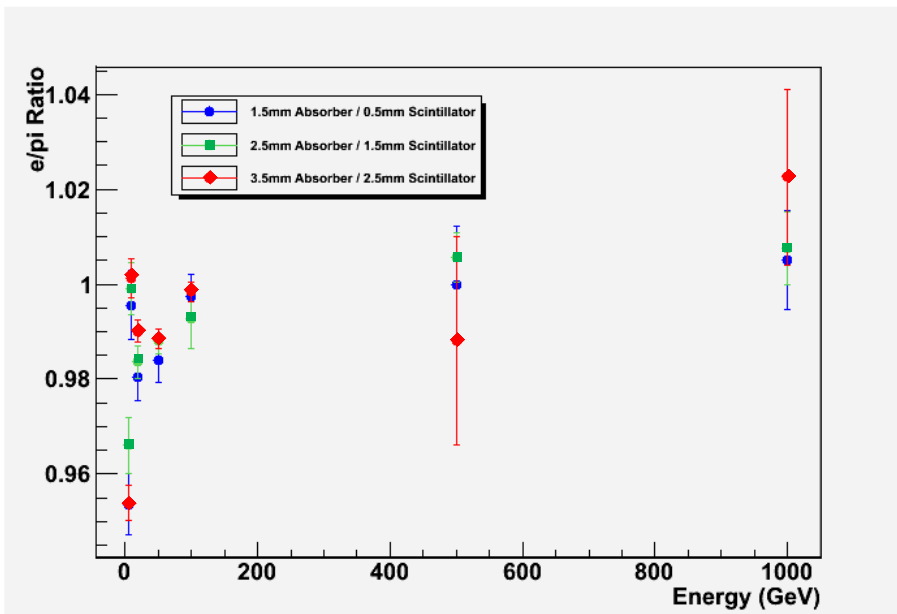

Figure 3.2: This plot displays the e/π ratio's dependence on energy. The three different colors correspond to different absorber and scintillator thicknesses. It can be seen that that there is a slight energy dependence.

Figure 3.2 shows the e/π ratio versus energy of the incident particles. It can be seen that larger energies tend to have ratios close to 1 but the range of ratios is very small. Even at low energies, the e/π ratio does not go below 0.94. Because this is the ratio of electron energy over pion energy, a lower ratio actually corresponds to the ECAL measuring hadronic particles better than electromagnetic ones. This slight decrease in the ratio is due to low energy electromagnetic particles losing more energy in the first few absorber layers. In other words, low energy electromagnetic particles lose a greater percentage of their energy in the absorber than low energy hadrons. In the endcap however, these low energy particles do not correspond to “interesting physics” and thus their energy measurements are not as critical. At CMS, interesting physics corresponds to particles with high transverse energy. This means that the Shashlik Detector has an e/π ratio close enough to 1 for all practical purposes meaning separate corrections for electromagnetic and hadronic particles will not be needed.

These results were unexpected because there are very few calorimeters with an e/π ratio so close to one and even fewer with ratio’s less than one. In order to verify these results, the same procedure was done with 0.1 mm of scintillating material and 40 mm of absorber. This resulted in a ratio’s no larger than 0.8 for high energy particles and lower than 0.4 for low energy particles. This behavior is to be expected so it seems that any discrepancies come from simplifications of the simulation as discussed above.

Ratio vs Absorber Thickness using 1.5mm Scintillator

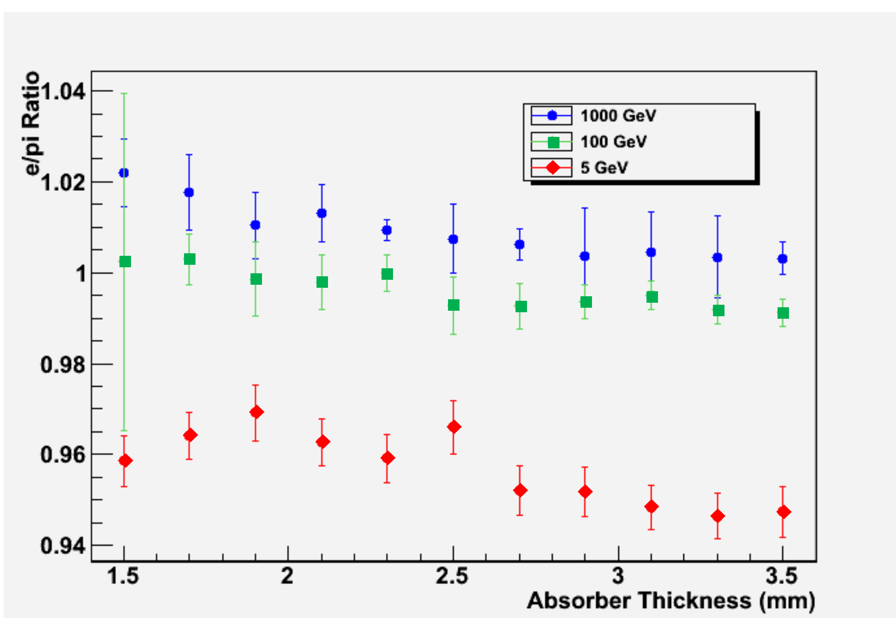

Figure 3.3: This plot displays the e/π ratio’s dependence on absorber layer thickness. The three different lines correspond to different energies. All data in plot was taken with a 1.5mm scintillator layers.

Ratio vs. Scintillator Thickness using 2.5mm Absorber

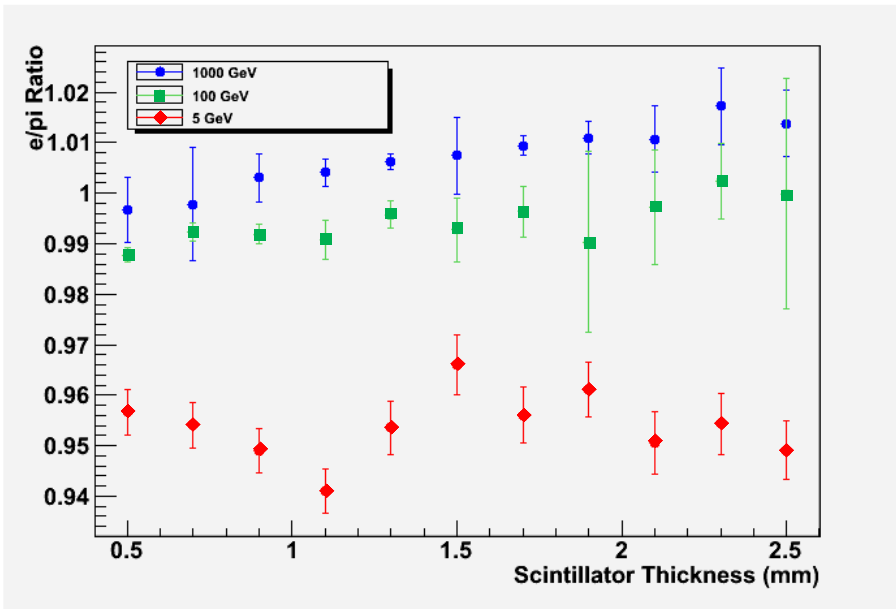

Figure 3.4: This plot displays the e/π ratio's dependence on scintillator layer thickness. The three different lines correspond to different energies. All data in plot was taken with 2.5mm absorber layers.

Figures 3.3 and 3.4 show the e/π ratio versus thicknesses of absorber and scintillator layers, respectively. This was done to determine if there is an optimal thickness ratio for use but the results indicate that this is unnecessary. Regardless of thickness, the Shashlik seems to have a fairly constant e/π ratio centered around 1. It follows that the e/π ratio need not be a concern when determining the thicknesses of the absorber and scintillating layers. Instead, the Shashlik can be optimized in terms of other quantities like cost and resolution.

e/π Ratio vs. Ratio of Scintillator to Absorber Materials

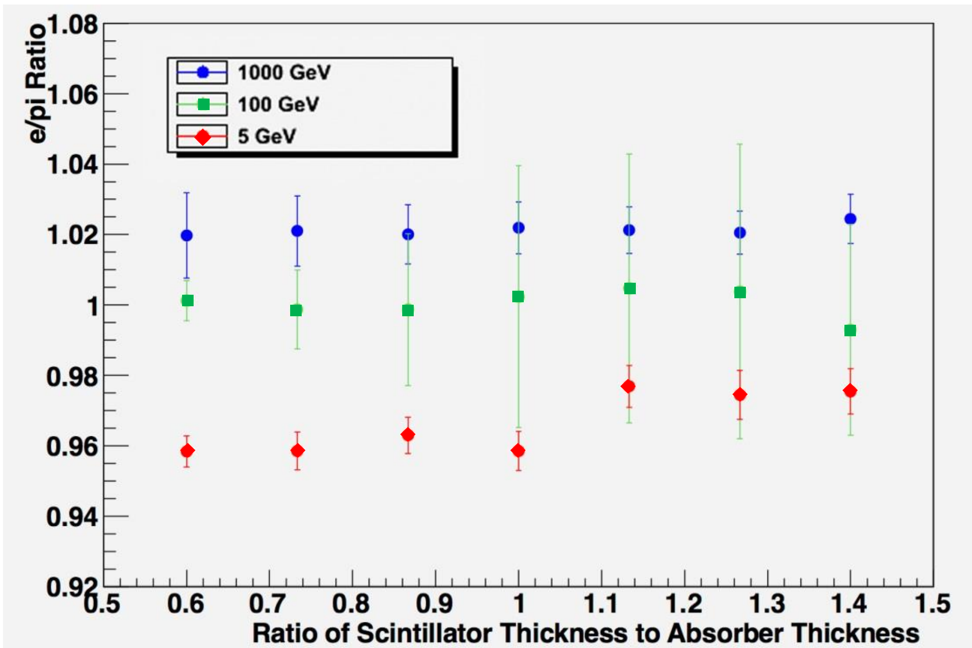

Figure 3.4: This plot displays the e/π ratio's dependence on the ratio of scintillator thickness to absorber thickness. The three different lines correspond to different energies.

To further demonstrate how little variance there is between absorber and scintillator thicknesses, Figure 3.4 plots the e/π ratio versus the ratio of scintillator thickness to absorber thickness for three different energies. Like in the previous plots, the lower energies have a slightly lower e/π ratio but the more important observation is that there is nearly zero slope for all data points. This further illustrates how little an effect the thicknesses have on the e/π ratio.

Part 4: Conclusion

Simulations were run using Pythia for particle generation and GEANT4 for detector simulation. The energies of 2000 electrons and 2000 pions were measured for varying energies and absorber/scintillator layer thicknesses. The ratio of these energies is commonly referred to as the e/π ratio. After analysis, it can be concluded that the e/π ratio for the Shashlik detector is close enough to the optimal value of 1 so that separate energy corrections will not be needed for electromagnetic and hadronic particles. The ratio can be seen versus energy in Figure 3.2. This graph shows that the ratio does drop a bit below 1 for low energies but these energies are largely irrelevant in the endcaps and are usually considered background noise. Figures 3.3 and 3.4 show the e/π ratio versus absorber and scintillator thicknesses and it can be seen that the thicknesses of these materials has even less of an effect on the ratio. To further demonstrate this, Figure 3.4 shows the e/π ratio versus the ratio of scintillator to absorber materials. Again, the ratio is largely centered around 1 and has very little variation. Fortunately, the combination of LYSO crystal and Tungsten absorber gives an e/π ratio of about 1 for all important energies and material thicknesses. Further studies could possibly include photon production at the simulation level and/or propagation of particles to confirm these results with a more realistic simulation.

References

1. Cms physics results. “CERN.” (2011, November 08). 10 Apr. 2014. <http://cms.web.cern.ch/news/cms-physics-results>

2. ATLAS Collaboration Georges Aad (Freiburg U.) et al. “Observation of a new particle in the search for the Standard Model Higgs boson with the ATLAS detector at the LHC.” Jul 2012. Phys.Lett. B716 (2012) 1-29

3. CERN. “What is cms?.” (2011, November 23) 10 Apr. 2014. < http://cms.web.cern.ch/news/what-cms>

4. Calorimetry for particle physics, C.W. Fabjan, F. Gianotti (CERN). Oct 2003. 96 pp. Published in Rev.Mod.Phys. 75 (2003) 1243-1286>

5. Ecal pictures and diagrams. (2010, August 24). 10 Apr. 2014. < https://cms-docdb.cern.ch/cgi-bin/PublicDocDB/ShowDocument?docid=2931>

6. Epic-Crystal. “Pbwo4 crystal.” (2010, August 24). 10 Apr. 2014. < http://www.epic-crystal.com/scintillationpbwo4crystal>

7. Kuske, T. ; Novotny, R.W. ; Schubert, R. “Browse Conference Publications > Nuclear Science Symposium and ... Help Working with Abstracts Radiation damage and recovery mechanisms in cooled PbWO4 crystals.” < http://citationmachine.net/index2.php>

8. Harvey Newman & Ren-Yuan Zhu. Presentation titled Preliminary Budget for Materials for Two LYSO Crystal Based Shashlik Matrices Each Composed of 25 Towers: Pb+LYSO and W+LYSO. March 27, 2013

9. CRC Handbook of Chemistry and Physics, CRC Press, 92nd Edition, 2011.

G. W. C. Kaye and T. H. Laby Tables of Physical and Chemical Constants, Longman, 16th Edition, 1995.

10. Omega Piezo. “Bgo, lyso and gso crystal scintillators.” n.d. 10 Apr. 2014. <http://www.omegapiezo.com/crystal_scintillators.html>

11. Atomic and Nuclear Properties of Materials: Tungsten. 20 Apr. 2014. <http://pdg.lbl.gov/2011/AtomicNuclearProperties/HTML_PAGES/074.html>

12. Lund University. “Pythia.” (2012) 10 Apr. 2014. <http://home.thep.lu.se/~torbjorn/Pythia.html>

13. GEANT4. (2014, March 21) 10 Apr. 2014. < http://GEANT4.cern.ch/>